Appl Magn Reson
DOI 10.1007/s00723-015-0729-5

Applied
Magnetic Resonance

Correlation of Signal Intensity and ICP/OES-Related Concentration of Gadolinium-based Nanomagnetic Particles in Molecular MRI: In Vitro Study

Banafsheh Nikfar[1] · Nader Riyahi Alam[1] · Soheila Haghgoo[2] · Hossein Ghanaati[3] · Hossein Ghanbari[4] · Mehdi Khoobi[5,6] · Behrooz Rafiei[3] · Ensiyeh Gorji[2] · Sara Heydarnezhadi[1]

Received: 29 June 2015 / Revised: 30 August 2015

Abstract Imaging methods have an important role in the management of patient's health care. Some of the advantages made magnetic resonance imaging (MRI) as an exclusive modality. Gd-DTPA is one of the most common contrast agents in clinical applications. In this study, the concentrations of three gadolinium-based MRI contrast agents were measured and quantification accuracy of these contrast agents by MRI method was investigated. Different concentrations from the Gd-DTPA, Gd_2O_3–DEG and paramagnetoliposome nanoparticles (encapsulated Gd_2O_3–DEG nanoparticles in liposome) samples were prepared. Physical characteristics of the contrast agents were investigated by DLS and TEM methods. The T_1-weighted images of the prepared samples were recorded using MRI scanner. For each sample, gadolinium concentrations were determined using the relaxation rates and relaxivities. Determined concentrations by the experimental and ICP/OES methods were

✉ Nader Riyahi Alam
riahialam@gmail.com

Banafsheh Nikfar
banafsheh.nikfar@gmail.com

1 Medical Physics and Biomedical Engineering Department, School of Medicine, Tehran University of Medical Sciences (TUMS), Tehran, Iran

2 Pharmaceutical Department, Food and Drug Laboratory Research Center, Food and Drug Organization (FDO), Ministry of Health, Tehran, Iran

3 Medical Imaging Center, Imam Hospital Complex, School of Medicine, Tehran University of Medical Sciences (TUMS), Tehran, Iran

4 Department of Medical Nanotechnology, School of Advanced Technologies in Medicine, Tehran University of Medical Sciences (TUMS), Tehran, Iran

5 Department of Medicinal Chemistry, Faculty of Pharmacy and Pharmaceutical Sciences Research Center, Tehran University of Medical Sciences (TUMS), Tehran, Iran

6 Medical Biomaterials Research Center, Tehran University of Medical Sciences (TUMS), Tehran, Iran

Published online: 14 October 2015

compared and the standard errors of the results were determined. Morphology, dimension and hydrodynamic diameter of the contrast agents were investigated. The hydrodynamic diameter of Gd_2O_3–DEG and PML nanoparticles were 90 ± 7.2 nm (with PdI = 0.328) and 96.8 ± 6.5 nm (with PdI = 0.299), respectively. In assessment of gadolinium concentrations, standard deviations of the experimental and ICP/OES data were ranged from 0.007 to 0.04. *P* values of all data points were higher than 0.05 that confirm there is no significant difference between the experimental and ICP/OES measurements. From the results, it could be concluded that MR systems could be used as an accurate and available method to estimate gadolinium concentrations.

1 Introduction

Imaging methods have an important role in the management of patient's health care [1–4]. Some of the advantages, such as excellent contrast for soft tissues, non-ionized radiations, and functional data acquisition, made magnetic resonance imaging (MRI) as an exclusive modality [3, 4]. Conventional MRI method provides morphological data that are used to investigate the abnormal deformities, bleeding, and many of other medical purposes. Contrast-enhanced MRI has more high sensitivity and specificity [24]. In tumoral lesions, accumulations of contrast agents were made by the abnormal functionality and angiogenesis. Therefore, contrast-based MR imaging was proposed to improve the lesion delectability. Positive (gadolinium based) or negative (iron based) contrast agents changed the relaxation rates (R_1 and R_2) of tissues. Different tissues could be differentiated by contrast-based MRI [4–10]. Gd-DTPA is one of the most common contrast agents in clinical applications. The gadolinium ions have odd electrons and they are toxic naturally, so they are used as chelates such as gadolinium-diethylenetriamine pentaacetic acid (Gd-DTPA). The new strategies based on nanomagnetic contrast probes were introduced to improve detectably of the targeted tissues in molecular MR imaging [10–18].

Molecular magnetic resonance imaging (mMRI) is a non-invasive technique to depict the biological procedures at the cellular and molecular dimensions. Early detection of diseases (i.e., cancers) could be possible using this method. Cellular functions and relevant molecular interactions could be diagnosed by the mMR imaging method immediately [14–22].

The contrast agents (iron or gadolinium based) should have appropriate features such as appropriate contrast enhancements, compatibility in the body and reactive surface for conjugating with biological active substance, accessibility and availability for medical situations. Super paramagnetic iron oxide (SPIO) is a nanoparticle contrast agent that enhances the signal intensity of T_2-weighted MRI images. Gadolinium-based contrast agents were also effective on T_1-weighted images [8–13].

The polymeric or lipidic biocompatible particles in the 3–350 nm range are appropriate for imaging applications. The nanoparticles in the smaller size of 100 nm increase relative surface and the predominant quantum confinement effects.

These properties of particles lead to incensement of reactivity ability and further linkage to functional matters. The proper coverage of magnetic nanoparticles could preserve their surface area from chemical reactions, oxidation of magnetic core and incensement of cellular uptake rate. Moreover, coating of nanoparticles could enhance half time of contrast agents and keep them from aggregation. Cell permeability and quality of nanomagnetic particle interactions with tissues are not exactly diaphanous [8–13]; hence, the concentration of nanoparticles should be specified in tissues.

In this study, the concentrations of three gadolinium-based MRI contrast agents [Gd-DTPA, Gd_2O_3–DEG and paramagnetoliposome nanoparticles (encapsulated Gd_2O_3–DEG nanoparticles in liposome)] were measured in a water phantom and quantification accuracy of these contrast agents by MRI method was investigated.

2 Materials and Methods

In this study, Gd-DTPA (Magnevist®) was prepared from Bayer Company (Germany). Gd_2O_3–DEG and paramagnetoliposome (PML) nanoparticles were synthesized and prepared at Food and Drug Laboratory Research Center [Food and Drug Organization (FDO), Ministry of Health, Tehran, Iran].

2.1 Gd_2O_3–DEG Nanoparticles Synthesis

Gd_2O_3 was prepared by polyol method [22, 23]. Hence, 2.5 mmol of $GdCl_3$-$6H_2O$ was dissolved at 12.5 mmol of Diethylene glycol (DEG) (Sigma-Aldrich Company) and then heated at 140 °C. Next, 3 mmol of NaOH was dissolved using 6 mmol of DEG and adjoined to the gadolinium containing solution. The solution was heated up to 180 °C and held under reflux and magnet stirrer about 4 h. The final product should be seemed as a dark yellow solution. After cooling process, the nanocrystals were filtered by 0.2 micron filter (polyethersulfone; Viva Science Sartorius, Hannover, Germany) and centrifuged at 2000 rpm at 40 °C for 30 min to isolate the agglomerated and large-size particles. Finally, Gd^{+3} free ions and extra Diethylene glycol was removed using 1000 Dalton dialysis membranes (Dialysis tubing cellulose membrane; Sigma-Aldrich) for 24 h across deionized water [23, 24].

2.2 Paramagnetoliposome (PML) Nanoparticles Synthesis

Liposomes were provided by lipid film hydration method. Therefore, 39.5 mg of 1, 2-Distearoyl-sn-glycero-3-phosphocholine (DSPC) (Lipoid GmbH, Germany) mixed to 19.35 mg of cholesterol (Sigma Company, Germany). 0.2 mmol of above mixture lipids was dissolved at 6 ml chloroform and 4 ml methanol. Then, it evaporated for 2 h to dryness by rotary evaporation at 65 °C and 80 rpm. Afterward, 2 mmol of Gd_2O_3–DEG was added to the lipid film and hydrated for 2 h. When paramagnetoliposome nanoparticles were formed, they should be sonicated for 30 min and dialyzed for 24 h across deionized water to remove non-encapsulated Gd_2O_3–DEG [22, 24].

Physical characteristics of the contrast agents (such as morphology and dimension) could be investigated by Dynamic Light Scattering (DLS) and Transmission Electron Micrographs (TEM) methods. The morphologies of the contrast agents could be depicted by TEM method. Dimension and diameter of the contrast agents could be also determined by DLS method [19, 21–25].

In this study, the prepared samples of the contrast agents were scanned by different methods. Dynamic Light Scattering, Transmission Electron Micrographs and Inductive Coupling Plasma/Optical Emission Spectrometry (ICP/OES) of the prepared samples were performed by Brookhaven, CM30 and PerkinElmer (Optima 7300 dv) systems, respectively.

Inductive Coupling Plasma/Optical Emission Spectrometry was considered as the gold standard method to determine the concentrations of gadolinium. Real concentrations of gadolinium were determined by the ICP/OES method.

2.3 Image Acquisition

Different concentrations of the Gd-DTPA, Gd_2O_3–DEG and paramegnetoliposome nanoparticles samples were prepared. The prepared samples were embedded in a water phantom for MR imaging. A schematic picture of the scanning setup is shown in Fig. 1. The T_1-weighted images were recorded using 1.5 Tesla MR scanner (GE–Signa Echospeed) with following parameters: Standard Spin Echo, Number of Echoes = 4, TE = 15 mSec, TR = 100, 200, 400, 600, 1000, 2000 and 3000 mSec, Matrix = 256 × 256, Slice Thickness = 4 mm, FOV = 25 cm, NEX = 1, Pixel Bandwidth = 15.

2.4 Data Analyzing

Concentration of contrast agents could also be determined by MRI method. In this method, concentration values were extracted by the following Eq. 1:

$$R_{1\,(\mathrm{obs})} = R_{1\,(\mathrm{int})} + r_1\,[C] \tag{1}$$

Fig. 1 Schematic picture of the scanning setup

where $R_{1\ (obs)}$ and $R_{1\ (int)}$ are the longitudinal relaxation rate of the contrast agents and water, respectively; r_1 is the longitudinal relaxivity and C is the gadolinium concentration [19, 21–24].

The signal intensities were extracted from the T_1-weighted MRI images of each sample [different concentration of the Gd-DTPA, Gd_2O_3–DEG and paramegnetoliposome (PML) nanoparticles]. The mean signal intensities (SI) were determined using MATLAB software (ver. 2008a, The MathWorks TM). In the written program, the mean pixel value from the 9 innermost pixels of each vial (ROI) was measured as the mean SI. Signal intensities vs. related TR values were plotted using Excel software (ver. 2010, Microsoft office). A linear line was fitted to these points using Excel software. The slope of this fitted line is the R_1 value for each sample.

The relaxation rates and relaxivities were replaced in the Eq. 1 and gadolinium concentrations were determined.

Determined concentrations by the experimental and ICP/OES methods were compared and the standard errors (SD) of the results were determined for these quantification methods.

3 Results and Discussion

Different concentrations of the Gd-DTPA, Gd_2O_3–DEG and paramagnetoliposome (PML) nanoparticles were scanned by MRI system. A T_1-weighted image of the samples is shown in Fig. 2. The numbers 1, 2, and 3 were used for different concentrations of the Gd-DTPA; 4, 5, 6 were used for different concentrations of the Gd_2O_3–DEG nanoparticles and 7, 8, 9 were used for different concentrations of the PML nanoparticles.

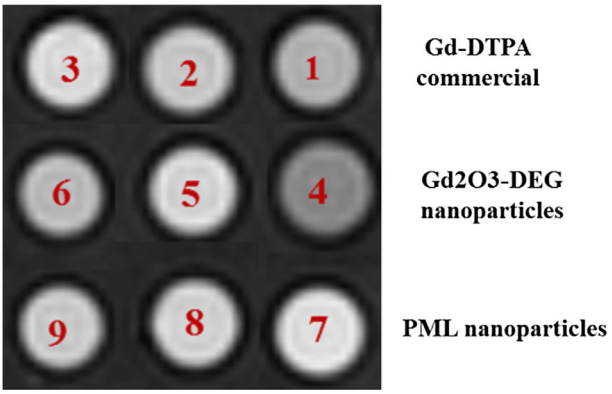

Fig. 2 Images of the Gd-DTPA, Gd_2O_3–DEG and PML nanoparticles samples by MRI (1.5 T) (*1*, *2*, *3* were used for different concentrations of the Gd-DTPA; *4*, *5*, *6* were used for different concentrations of the Gd_2O_3–DEG nanoparticles and *7*, *8*, *9* were used for different concentrations of the PML nanoparticles)

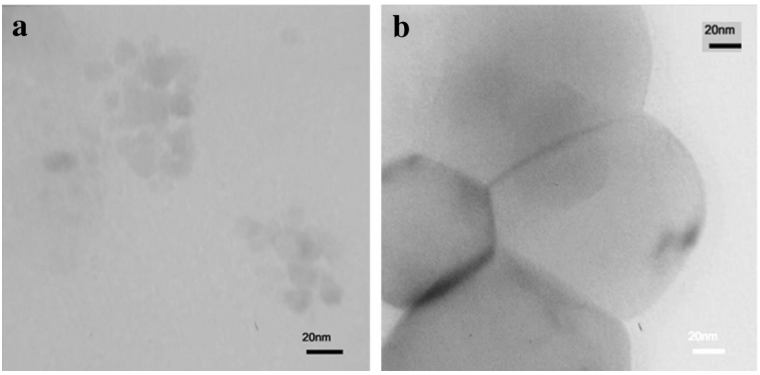

Fig. 3 **a** TEM image of the Gd_2O_3–DEG nanoparticles. **b** TEM image of the PML nanoparticles

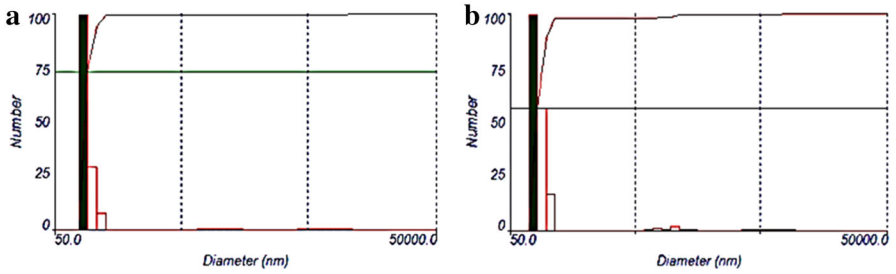

Fig. 4 **a** DLS result of the Gd_2O_3–DEG nanoparticles with hydrodynamic diameter = 90 ± 7.2 nm. **b** DLS result of the PML nanoparticles with hydrodynamic diameter = 96.8 ± 6.5 nm

Morphology, dimension and diameter of the contrast agents (as the physical characteristics) were investigated. The morphologies of the Gd_2O_3–DEG and PML nanoparticles were depicted by TEM method. The images of the Gd_2O_3–DEG and PML morphologies (in 20 nm scale) are shown in Fig. 3.

The scanning results of the DLS method for the nanocontrast agents are indicated in Fig. 4. According to the DLS results, the hydrodynamic diameter of Gd_2O_3–DEG and PML nanoparticles were 90 ± 7.2 nm (with PdI = 0.328) and 96.8 ± 6.5 nm (with PdI = 0.299), respectively. Determined diameters of the Gd_2O_3–DEG and PML nanoparticles were in good agreements with that of other studies [19, 21–24].

For each sample of the contrast agents, signal intensities vs. related TR values were plotted by EXCEL software. The obtained graphs are called longitudinal relaxation time or T_1 curve. T_1 curves of the Gd-DTPA, Gd_2O_3–DEG and PML nanoparticles in different concentrations (the numbers 1–9) are plotted in Fig. 5. The slope of the T_1 curve indicates longitudinal relaxation rate (R_1) that the inverse of longitudinal relaxation rate is longitudinal relaxation time (T_1). T_1 value was calculated by MATLAB software (ver. 2011) based on the Eq. 2 [26, 27]

$$S = \mathrm{PD}\left(1 - e^{-\mathrm{TR}/T_1}\right)e^{-\mathrm{TE}/T_2} \tag{2}$$

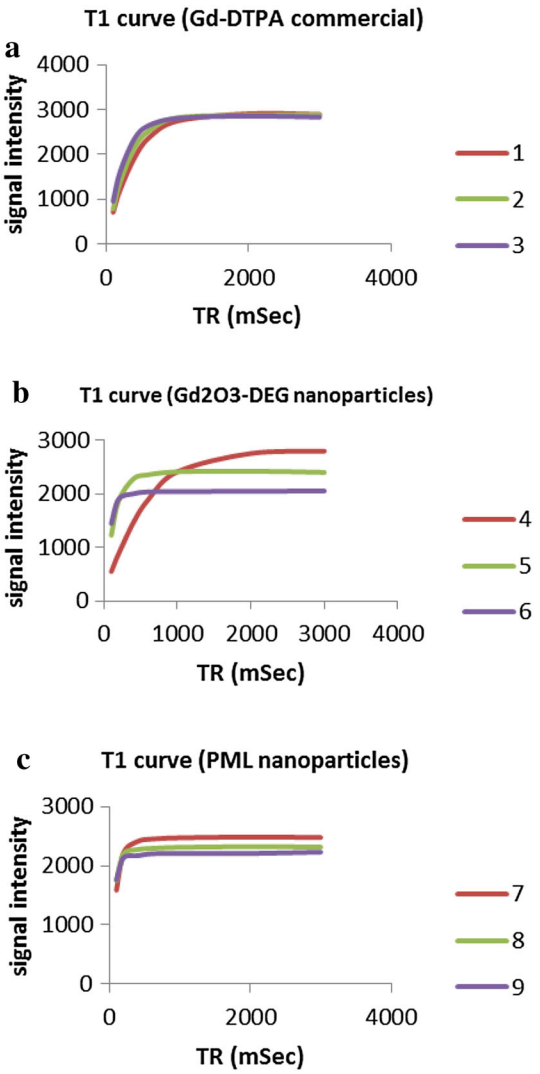

Fig. 5 T_1 curves for different concentrations of the **a** Gd-DTPA, **b** Gd_2O_3–DEG nanoparticles, **c** PML nanoparticles (the numbers *1–9* in the figure were used for different concentrations of the contrast agents)

where S is signal intensity, PD is proton density, TR is time repetition and TE is echo time. For each sample, the determined (MRI method) and measured (ICP/OES method) concentrations were compared. Accuracy and standard deviation of the results were also investigated and determined. The obtained concentrations for the Gd-DTPA, Gd_2O_3–DEG and PML nanoparticles are depicted in Fig. 6 (the numbers 1–9 were used for different concentrations of the contrast agents that was explained before in Fig. 2).

Standard deviations of the experimental and ICP/OES data were ranged from 0.007 to 0.04. P values of all data points were higher than 0.05 that confirm there is no significant difference between the experimental and ICP/OES measurements.

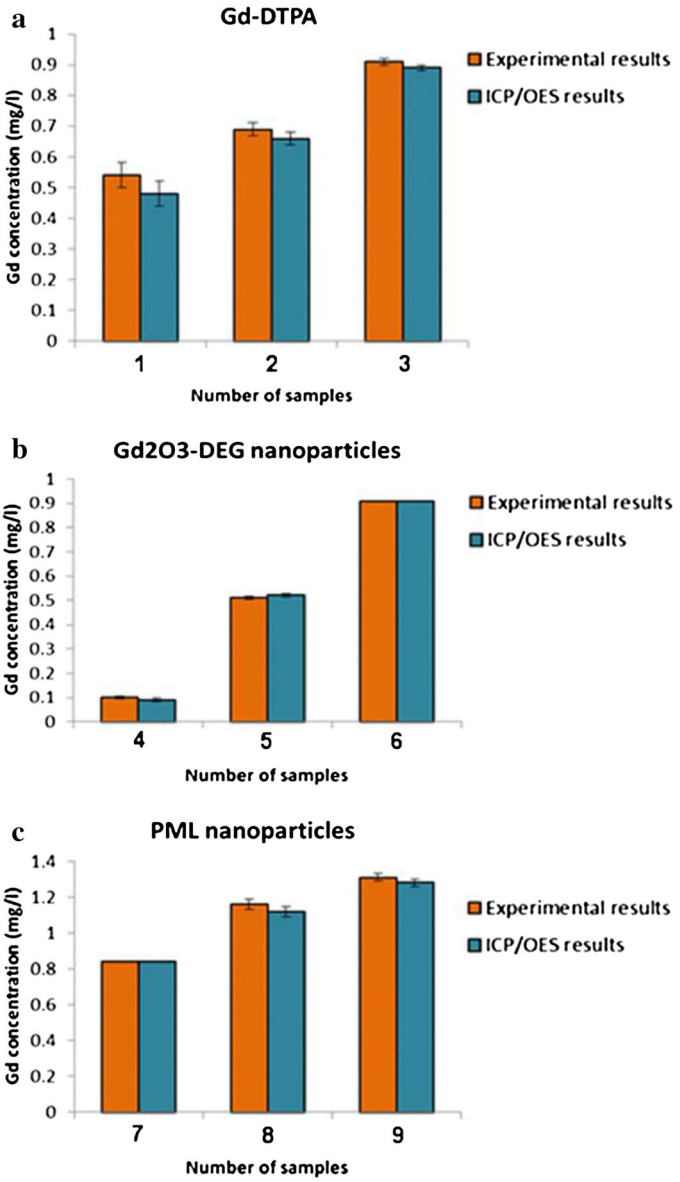

Fig. 6 Experimental and ICP/OES results of the determined gadolinium concentrations for **a** Gd-DTPA samples, **b** PML samples and **c** Gd_2O_3–DEG samples (along with ±SD) (The numbers of *1* to *9* in the figure were used for different concentrations of the contrast agents)

In the present study, different concentrations of gadolinium-based contrast agents were evaluated in a water phantom, but it could also be used in ex vivo and in vivo situations. Assessment of gadolinium concentrations in cells and live tissues could be helpful for better understanding of lesions.

4 Conclusion

Gadolinium-based nanomagnetic particles are extensively selected for the large magnetic moment and fine magnetic features, due to their unpaired electrons. Thus, selection of a suitable biocompatible coverage for magnetic nanoparticles could improve relaxivity and half-life of the MR contrast agents. In this study, gadolinium concentrations were estimated accurately (with high precision) for different concentrations of the gadolinium-based MRI contrast agents in water solutions. So, routine clinical MRI systems could be applied as an accurate, accessible and practical procedure to estimate gadolinium concentrations in vitro.

Acknowledgments Our thanks to Food and Drug Laboratory Research Center and Imam Khomeini Hospital for their supports. Also, the authors appreciate Dr.Faraz Kalantari and Dr.Salman Zakariaee for the paper revision.

References

1. M. R. Bashir, *Hepatobiliary Imaging: Magnetic Resonance Contrast Agents for Liver Imaging* (Elsevier Health Sciences, 2013), pp. 1–249
2. Medical Imaging for improved patient care. European Science Foundation policy briefing (2007)
3. L. Telgmann, M. Sperling, U. Karst, Anal. Chim. Acta **764**, 1–16 (2013)
4. Z. Zhou, L. Zheng-Rong, Wiley Interdiscip. Rev. Nanomed. Nanobiotechnol. **5**(1), 1–18 (2013)
5. P. Caravan, J.J. Ellison, T.J. McMurry, R.B. Lauffer, Chem. Rev. **99**, 2293–2352 (1999)
6. Y. Zhang, N. Kohler, M. Zhang, Biomaterials **23**, 1553–1561 (2002)
7. P. Caravan, Chem. Soc. Rev. **35**, 512–523 (2006)
8. S. Laurent, L.V. Elst, R.N. Muller, Contrast Media Mol. Imaging **1**, 128–137 (2006)
9. G. Schuhmanngiampieri, H. Schmittwillich, T. Frenzel, W.R. Press, H.J. Weinmann, Invest. Radiol. **26**, 969–974 (1991)
10. N. Kamaly, A.D. Miller, J.D. Bell, Curr. Top. Med. Chem. **10**, 1158–1183 (2010)
11. H.J. Weinmann, R.C. Brasch, W.R. Press, G.E. Wesbey, Am. J. Roentgenol. **142**, 619–624 (1984)
12. M. Port, C. Corot, O. Rousseaux, I. Raynal, L. Devoldere, J.M. Idee, A. Dencausse, S. Le Greneur, C. Simonot, D. Meyer, Magn. Reson Mater. Phy. Biol. Med. **12**, 121–127 (2001)
13. E. Waters, S. Wickline, Basic Res. Cardiol. **103**, 114–121 (2008)
14. A. Hengerer, J. Grimm, Biomed. Imaging Interv. J. **2**(2), 1–7 (2006)
15. G.M. Lanza, P.M. Winter, S.D. Caruthers, A.M. Morawski, A.H. Schmieder, K.C. Crowder, S.A. Wickline, J. Nucl. Cardiol. **11**(6), 733–743 (2004)
16. B. Gimi, Proc. IEEE Inst. Electr. Electron Eng. **93**(4), 784–799 (2005)
17. D. Artemov, J. Cell. Biochem. **90**, 518–524 (2003)
18. J.C. Gore, H.C. Manning, C.C. Quarles, K.W. Waddell, T.E. Yankeelov, Magn. Reson. Imaging **29**, 587–600 (2011)
19. N. Riyahi-Alam, Z. Behrouzkia, A. Seifalian, S.H. Jahromi, Biol. Trace Elem. Res. **137**(3), 324–334 (2010)
20. H.B. Na, I.C. Song, T. Hyeon, Adv. Mater. **21**(21), 2133–2148 (2009)
21. S. Riyahi-Alam, S. Haghgoo, E. Gorji, N. Riyahi-Alam, Iran. J. Pharm. Res. **14**(1), 3 (2015)
22. R. Zohdiaghdam, N. Riyahi-Alam, H.R. Moghimi, S. Haghgoo, A. Alinaghi, G. Azizian, B. Rafiei, J. Microencapsul. **30**(7), 613–623 (2013)
23. G. Azizian, N. Riyahi-Alam, S. Haghgoo, M. Saffari, R. Zohdiaghdam, E. Gorji, Mater. Sci. Pol. **31**(2), 158–164 (2013)
24. G. Azizian, N. Riyahi-Alam, S. Haghgoo, H.R. Moghimi, R. Zohdiaghdam, B. Rafiei, E. Gorji, Nanoscale Res. Lett. **7**(1), 1–10 (2012)
25. B.J. Berne, R. Pecora, *Dynamic Light Scattering: With Applications to Chemistry, Biology, and Physics* (Courier Dover Publications, USA, 2000), pp. 38–53

26. B. Carrero-González, M.T. De La Cruz, M.A. Casermeiro, J. Soil Sci. Plant Nutr. **12**(1), 165–182 (2012)
27. G.E. Gold, E. Han, J. Stainsby, G. Wright, J. Brittain, C. Beaulieu, Am. J. Roentgenol. **183**(2), 343–351 (2004)